SIAM J. NUMER. ANAL.
Vol. 55, No. 2, pp. 737–757

VARIATIONAL FORMULATION AND NUMERICAL ANALYSIS OF LINEAR ELLIPTIC EQUATIONS IN NONDIVERGENCE FORM WITH CORDES COEFFICIENTS*

DIETMAR GALLISTL†

Abstract. This paper studies formulations of second-order elliptic partial differential equations in nondivergence form on convex domains as equivalent variational problems. The first formulation is that of Smears and Süli [*SIAM J. Numer. Anal.*, 51 (2013), pp. 2088–2106], and the second one is a new symmetric formulation based on a least-squares functional. These formulations enable the use of standard finite element techniques for variational problems in subspaces of H^2 as well as mixed finite element methods from the context of fluid computations. Besides the immediate quasi-optimal a priori error bounds, the variational setting allows for a posteriori error control with explicit constants and adaptive mesh-refinement. The convergence of an adaptive algorithm is proved. Numerical results on uniform and adaptive meshes are included.

Key words. finite element methods, Cordes coefficients, nondivergence form, fourth order, variational formulation, adaptive algorithm

AMS subject classifications. 31B30, 35J30, 65N12, 65N15, 65N30

DOI. 10.1137/16M1080495

1. Introduction.

Let $\Omega \subseteq \mathbb{R}^d$ be an open, bounded, convex polytope for $d \in \{2,3\}$. This article deals with the numerical approximation of strong solutions $u \in H^1_0(\Omega) \cap H^2(\Omega)$ to the second-order elliptic partial differential equation (PDE)

$$L(u) = f \quad \text{in } \Omega \qquad u = 0 \quad \text{on } \partial\Omega, \tag{1}$$

where $f \in L^2(\Omega)$ is a given square-integrable function and the operator L has nondivergence form. More precisely, it is given through

$$L(v) := A : D^2 v := \sum_{j,k=1}^{d} A_{jk} \partial^2_{jk} v \qquad \text{for any } v \in V := H^1_0(\Omega) \cap H^2(\Omega). \tag{2}$$

In the case that the coefficient A satisfies certain smoothness assumptions, it is known that (1) can be converted into a second-order equation in divergence form through the product rule. If A is merely an essentially bounded tensor, such a reformulation is not valid and variational formulations of (1) are less obvious. It is proved in [21] that the unique solvability is assured through the Cordes condition [6, 16] described in section 2 below. The first fully analyzed numerical scheme suited for L^∞ Cordes coefficients was suggested and analyzed in [21] and belongs to the class of discontinuous Galerkin methods. It was successfully applied in [22, 23] to fully nonlinear Hamilton–Jacobi–Bellman equations. Further works on discontinuous Galerkin methods for nondivergence form problems [9, 10] focus on error estimates in $W^{k,p}$ norms for the case of continuous coefficients. Other approaches include the discrete Hessian

*Received by the editors June 20, 2016; accepted for publication (in revised form) January 13, 2017; published electronically March 28, 2017.
http://www.siam.org/journals/sinum/55-2/M108049.html
Funding: The work of the author was funded by Deutsche Forschungsgemeinschaft (DFG) through CRC1173.
†Institut für Angewandte und Numerische Mathematik, Karlsruher Institut für Technologie, D-76131 Karlsruhe, Germany (gallistl@kit.edu).

method of [14] and the two-scale method of [19]. The latter work is based on the integro-differential approach of [4] and focuses on L^∞ error estimates.

This paper studies variational formulations of (2) for the case of discontinuous coefficients satisfying the Cordes condition. The formulation seeks $u \in V$ such that

$$(A : D^2 u, \tau(\nabla v))_{L^2(\Omega)} = (f, \tau(\nabla v))_{L^2(\Omega)} \quad \text{for all } v \in V,$$

where the operator $\tau : H^1(\Omega; \mathbb{R}^d) \to L^2(\Omega)$ acts on the test functions. In this work, two possible options are discussed. The choice $\tau = \tau^{\mathrm{NS}} := \gamma \operatorname{div} \bullet$ (for the function γ defined in (5) below) leads to the nonsymmetric formulation of [21]. The second possibility is $\tau = \tau^{\mathrm{LS}} := A : D\bullet$ which results in a symmetric problem that turns out to be the Euler–Lagrange equation for the minimization of the functional $\|A : D^2 v - f\|^2_{L^2(\Omega)}$. The superscripts NS and LS stand for "nonsymmetric" and "least-squares," respectively, owing to the properties of the individual method. The variational formulations naturally allow the use of C^1-conforming finite element methods [5]. Since C^1 finite elements are sometimes considered impractical, alternative discretization techniques are desirable. We apply the recently proposed mixed formulation [11] to the present problem. Its formulation involves function spaces similar to those employed for the Stokes equations. In the sense of the least-squares functional, the minimization problem is restated as the minimization of $\|A : D\phi - f\|^2_{L^2(\Omega)}$ over all vector-valued H^1 functions with vanishing tangential trace subject to the constraint that $\operatorname{rot} \phi = 0$. While the continuous formulations are equivalent, the latter can be discretized with H^1-conforming finite elements in the framework of saddle-point problems [2, 11]. In the discrete formulation, the structure of the differential operator requires the incorporation of an additional stabilization term. This is mainly due to the fact that $L(v)$ in the L^2 norm is bounded from below by the norm of the Laplacian Δv rather than the full Hessian tensor $D^2 v$. This is also the reason why the application of nonconforming schemes is not as immediate as for the usual biharmonic equation. Indeed, nonconforming finite element spaces may contain piecewise harmonic functions, and thus, it is not generally possible to bound the piecewise Laplacian from below by the piecewise Hessian unless further stabilization terms are included. For example, the divergence theorem readily implies that three out of the six local basis function of the Morley finite element [5] are harmonic. The conforming and mixed finite element formulations presented here lead to quasi-optimal a priori error estimates and give rise to natural a posteriori error estimates based on strong L^2 volume residuals where on any element of the finite element partition the residual reads $\|A : D^2 u_h - f\|^2_{L^2(T)}$ for the conforming finite element solution u_h (with an analogous formula for the mixed discretization). Since this residual equals $\|A : D^2(u_h - u)\|^2_{L^2(T)}$, it immediately leads to reliable and efficient estimates with explicit constants (depending solely on the data). This error estimator can be employed for guiding a self-adaptive refinement procedure. This work focuses on h-adaptivity and does not address a local adaptation of the polynomial degree as in [21]. For the suggested class of discretizations, the convergence of the adaptive algorithm can be proved. Since the proof utilizes a somehow indirect argument (similar to that of [17]), no convergence rate is obtained. The performance of the adaptive mesh-refinement procedure is numerically studied in the experiments of this paper.

The remaining parts of this article are as follows: section 2 revisits the unique solvability results of [21] and presents the variational formulations; section 3 presents the a priori and a posteriori error estimates for finite element discretizations. The convergence analysis of an adaptive algorithm follows in section 4. Numerical experiments are presented in section 5. The remarks of section 6 conclude the paper.

Standard notation on function spaces applies throughout this article. Lebesgue and Sobolev functions with values in $\mathbb{R}^d$ are denoted by $L^2(\Omega;\mathbb{R}^d)$, $H^1(\Omega;\mathbb{R}^d)$, etc. The $d\times d$ identity matrix is denoted by $I_{d\times d}$. The inner product of real-valued $d\times d$ matrices A, B is denoted by $A:B=\sum_{j,k=1}^d A_{jk}B_{jk}$. The Frobenius norm of a $d\times d$ matrix A is denoted by $|A|:=\sqrt{A:A}$; the trace reads $\operatorname{tr} A$. For vectors, $|\cdot|$ refers to the Euclidean length. The rotation (often referred to as $\operatorname{curl} v$ or $\nabla\wedge v$) of a vector field v is denoted by $\operatorname{rot} v$. The union of a collection $\mathcal{X}$ of subsets of $\mathbb{R}^d$ is indicated by the symbol $\cup$ without index and reads $\cup\mathcal{X}:=\{x\in\mathbb{R}^d : x\in X \text{ for some } X\in\mathcal{X}\}$.

2. Problem setting and variational formulations. This section lists some conditions for the unique solvability of (1) and proceeds with the variational formulations. Throughout this article it is assumed that the coefficient $A\in L^\infty(\Omega;\mathbb{R}^{d\times d})$ is uniformly elliptic, that is, there exist constants $0<\alpha_1\le\alpha_2<\infty$ such that

$$\alpha_1\le\inf_{\xi\in\mathbb{R}^d,|\xi|=1}\xi^*A\xi\le\sup_{\xi\in\mathbb{R}^d,|\xi|=1}\xi^*A\xi\le\alpha_2\quad\text{almost everywhere in }\Omega. \tag{3}$$

Assume furthermore that there exists some $\varepsilon\in(0,1]$ such that

$$|A|^2/(\operatorname{tr}A)^2\le 1/(d-1+\varepsilon)\quad\text{almost everywhere in }\Omega. \tag{4}$$

Assumption (4) is called the *Cordes condition* [6, 16, 21]. Define the function γ by

$$\gamma:=\operatorname{tr}(A)/|A|^2. \tag{5}$$

While in the planar case, $d=2$, the Cordes condition is implied by (3); it is an essential condition for $d\ge 3$ and its absence may lead to ill-posedness of the PDE (1) [16, 20]. The uniform ellipticity (3) implies that γ is uniformly bounded from below by some positive constant γ_0 [21]. The following result can be found in [16, 21].

LEMMA 2.1. *Let $A\in L^\infty(\Omega;\mathbb{R}^{d\times d})$ satisfy* (3) *and* (4). *Then, almost everywhere in Ω, the following estimate holds for any $B\in\mathbb{R}^{d\times d}$,*

$$|(\gamma A-I_{d\times d}):B|=|\gamma A:B-\operatorname{tr}B|\le\sqrt{1-\varepsilon}\,|B|$$

as well as $|\gamma A-I_{d\times d}|\le\sqrt{1-\varepsilon}$.

Proof. See, e.g., the proof of [21, Lemma 1]. ∎

The triangle inequality shows that A almost everywhere satisfies for any $B\in\mathbb{R}^{d\times d}$

$$\gamma|A:B|\ge|\operatorname{tr}B|-|(\gamma A-I_{d\times d}):B|. \tag{6}$$

The space of H^1 vector fields with vanishing tangential trace reads

$$W:=\{v\in H^1(\Omega;\mathbb{R}^d) : \text{the tangential trace of } v \text{ on } \partial\Omega \text{ vanishes}\}. \tag{7}$$

For the analysis of the formulations below, it it is useful to note that, on convex domains, the following estimate holds [7, Thm. 2.3]:

$$\|Dw\|_{L^2(\Omega)}^2\le\|\operatorname{rot}w\|_{L^2(\Omega)}^2+\|\operatorname{div}w\|_{L^2(\Omega)}^2\quad\text{for any } w\in W \tag{8}$$

(on polytopes even with equality). For any $w\in W$ with $\operatorname{rot}w=0$, the combination of (6) for $B=Dw$ with Lemma 2.1 and (8) results in

$$\|\gamma A:Dw\|_{L^2(\Omega)}\ge(1-\sqrt{1-\varepsilon})\,\|\operatorname{div}w\|_{L^2(\Omega)}\ge(1-\sqrt{1-\varepsilon})\,\|Dw\|_{L^2(\Omega)}. \tag{9}$$

Similar calculations (already carried out in [21]) with Lemma 2.1 and (8) prove for any $w \in W$ with $\operatorname{rot} w = 0$ that

$$(A : Dw, \gamma \operatorname{div} w)_{L^2(\Omega)} = \|\operatorname{div} w\|^2_{L^2(\Omega)} + ((\gamma A - I_{d\times d}) : Dw, \operatorname{div} w)_{L^2(\Omega)} \\ \geq (1 - \sqrt{1-\varepsilon})\|\operatorname{div} w\|^2_{L^2(\Omega)} \geq (1 - \sqrt{1-\varepsilon})\|Dw\|^2_{L^2(\Omega)}. \tag{10}$$

We proceed with the description of the variational setting. Define the space $V := H^1_0(\Omega) \cap H^2(\Omega)$. An application of (8) shows that the L^2 norm of the Hessian of any $v \in V$ is controlled by the norm of the Laplacian [7, 13, 21]

$$\|D^2 v\|_{L^2(\Omega)} \leq \|\Delta v\|_{L^2(\Omega)} \quad \text{for any } v \in V. \tag{11}$$

Define the operators $\tau^{\mathrm{NS}}, \tau^{\mathrm{LS}} : H^1(\Omega; \mathbb{R}^d) \to L^2(\Omega)$ by

$$\tau^{\mathrm{NS}}(\phi) := \gamma \operatorname{div} \phi \quad \text{and} \quad \tau^{\mathrm{LS}}(\phi) := A : D\phi \qquad \text{for any } \phi \in H^1(\Omega; \mathbb{R}^d).$$

As mentioned in the introduction, each of these operators corresponds to a specific choice of test functions in a variational formulation and thus constitutes a class of numerical methods. The variational problem seeks $u \in V$ such that

$$(A : D^2 u, \tau(\nabla v))_{L^2(\Omega)} = (f, \tau(\nabla v))_{L^2(\Omega)} \quad \text{for all } v \in V \tag{12}$$

for $\tau = \tau^{\mathrm{NS}}$ (the nonsymmetric formulation of [21]) or $\tau = \tau^{\mathrm{LS}}$ (the least-squares formulation proposed here). The lower bound (10) with $w = \nabla v$ implies that (12) is coercive for $\tau = \tau^{\mathrm{NS}}$. The lower bound (9) with $w = \nabla v$ implies for any $v \in V$ that

$$\|\gamma\|^2_{L^\infty(\Omega)}(A : D^2 v, \tau^{\mathrm{LS}}(\nabla v))_{L^2(\Omega)} \geq \|\gamma A : D^2 v\|^2_{L^2(\Omega)} \geq (1 - \sqrt{1-\varepsilon})^2 \|D^2 v\|^2_{L^2(\Omega)}.$$

Thus, $(A : D^2 \bullet, A : D^2 \bullet)_{L^2(\Omega)}$ is an inner product on V with

$$\|A : D^2 v\|_{L^2(\Omega)} \geq c(\gamma, \varepsilon)\|D^2 v\|_{L^2(\Omega)} \quad \text{for any } v \in V, \tag{13}$$

$$\text{where} \qquad c(\gamma, \varepsilon) := (1 - \sqrt{1-\varepsilon})/\|\gamma\|_{L^\infty(\Omega)}. \tag{14}$$

This yields well-posedness of (12) for $\tau = \tau^{\mathrm{LS}}$. The following result proves the equivalence of (1) and (12).

PROPOSITION 2.2. *Let $\tau = \tau^{\mathrm{NS}}$ or $\tau = \tau^{\mathrm{LS}}$. A function $u \in V$ solves* (1) *strongly in $L^2(\Omega)$ if and only if it solves the variational form* (12).

Proof. For the choice $\tau = \tau^{\mathrm{NS}}$, the assertion was proved in [21, proof of Thm. 3], and it remains to consider the case $\tau = \tau^{\mathrm{LS}}$. It is immediate that (1) implies (12). For the converse direction it is enough to note that (12) is the Euler–Lagrange equation of the convex minimization problem

$$u \in \operatorname*{arg\,min}_{v \in V} \|A : D^2 v - f\|^2_{L^2(\Omega)}. \tag{15}$$

Since (3) and (4) imply that (1) is uniquely solvable on convex domains [21], this establishes the equivalence. ∎

Formulation (12) is variational and thus suited for approximation with the finite element method (FEM). Standard finite elements will be discussed in subsection 3.1. Since the construction of H^2-conforming finite elements is rather cumbersome, mixed

formulations appear as an attractive alternative. To state the mixed formulation recently proposed in [11], recall the definition of W from (7) and define the space

$$Q := \begin{cases} \{q \in L^2(\Omega) : \int_\Omega q\,dx = 0\} & \text{if } d = 2, \\ \{q \in L^2(\Omega;\mathbb{R}^3) : \operatorname{div} q = 0 \text{ in } \Omega \text{ and } q \cdot \nu|_{\partial\Omega} = 0 \text{ on } \partial\Omega\} & \text{if } d = 3. \end{cases}$$

Here ν denotes the outer unit normal of the domain Ω. Define the bilinear forms $a_\tau : W \times W \to \mathbb{R}$ (for $\tau = \tau^{\mathrm{NS}}$ or $\tau = \tau^{\mathrm{LS}}$) and $b : W \times Q \to \mathbb{R}$ by

$$\begin{aligned} a_\tau(v,z) &:= (A : Dv, \tau(z))_{L^2(\Omega)} && \text{for any } (v,z) \in W \times W, \\ b(v,q) &:= (\operatorname{rot} v, q)_{L^2(\Omega)} && \text{for any } (v,q) \in W \times Q. \end{aligned}$$

The mixed formulation of (12) is to seek $(u,w,p) \in H^1_0(\Omega) \times W \times Q$ such that

$$(\nabla u - w, \nabla z)_{L^2(\Omega)} = 0 \qquad \text{for all } z \in H^1_0(\Omega), \tag{16a}$$

$$a_\tau(w,v) + b(v,p) = (f, \tau(v))_{L^2(\Omega)} \qquad \text{for all } v \in W, \tag{16b}$$

$$b(w,q) = 0 \qquad \text{for all } q \in Q. \tag{16c}$$

For the analysis of the well-posedness of (16b)–(16c), recall estimate (10) for $\tau = \tau^{\mathrm{NS}}$ and (9) for $\tau = \tau^{\mathrm{LS}}$, which imply that the form a_τ is coercive on the subspace of W consisting of rotation-free vector fields, namely, for all $v \in W$ with $\operatorname{rot} v = 0$,

$$\begin{aligned} (1 - \sqrt{1-\varepsilon})\|Dv\|^2_{L^2(\Omega)} \le a_{\tau^{\mathrm{NS}}}(v,v) \le \|A\|_{L^\infty(\Omega)}\|\gamma\|_{L^\infty(\Omega)}\|Dv\|^2_{L^2(\Omega)}, \\ c(\gamma,\varepsilon)^2\|Dv\|^2_{L^2(\Omega)} \le a_{\tau^{\mathrm{LS}}}(v,v) \le \|A\|^2_{L^\infty(\Omega)}\|Dv\|^2_{L^2(\Omega)}. \end{aligned} \tag{17}$$

Since there exists a constant $\beta > 0$ such that the following inf-sup condition is valid,

$$\beta \le \inf_{q \in Q\setminus\{0\}} \sup_{v \in W\setminus\{0\}} b(v,q) \big/ (\|Dv\|_{L^2(\Omega)}\|q\|_{L^2(\Omega)}), \tag{18}$$

problem (16b)–(16c) (and thus (16)) is uniquely solvable [2]. The stability (18) (employed in [11]) is based on a regularized decomposition given in [15], which is stronger than the classical Helmholtz decomposition [12].

PROPOSITION 2.3. *Let $\tau = \tau^{\mathrm{NS}}$ or $\tau = \tau^{\mathrm{LS}}$. Problems* (12) *and* (16) *are equivalent in the following sense. If $u \in V$ solves* (12)*, then there exists $p \in Q$ such that $(u, \nabla u, p)$ solves* (16)*. If, conversely, $(u,w,p) \in H^1_0(\Omega) \times W \times Q$ solves* (16)*, then u belongs to V and solves* (12) *with $w = \nabla u$.*

Proof. The proof is essentially contained in [11]. For completeness, it is sketched here. It is easily verified that $w := \nabla u$ is rotation-free, i.e., $\operatorname{rot} w = 0$. By (18) there exists a Lagrange multiplier $p \in Q$ such that system (16) is satisfied. Let, conversely, w satisfy (16b)–(16c). Since $\operatorname{rot} w = 0$ and Ω is convex, there exists a potential $\phi \in H^1_0(\Omega)$ with $\nabla\phi = w$. By (16a), the difference $u - \phi$ satisfies the homogeneous Laplace equation with zero Dirichlet conditions, and hence $u = \phi$ and $w = \nabla u$. ∎

Remark 1. It is not difficult to see that the Lagrange multiplier p equals zero in the continuous setting. This property will not be preserved by typical discretizations.

Remark 2. In the case that the operator L has the form (2), the system (16) decouples into a Stokes-type problem plus the postprocessing for the primal variable. For more general equations involving zeroth-order terms, see the comments in section 6.

3. Finite element discretization. This section presents conforming and mixed finite element discretizations and their error analysis for the problems of section 2.

3.1. Conforming discretization. The variational formulation (12) immediately allows stable discrete formulations with conforming finite elements. Let $V_h \subseteq V$ be a closed subspace. The discrete problem is to seek $u_h \in V_h$ such that

$$(A : D^2 u_h, \tau(\nabla v_h))_{L^2(\Omega)} = (f, \tau(\nabla v_h))_{L^2(\Omega)} \quad \text{for all } v_h \in V_h \tag{19}$$

for $\tau = \tau^{\mathrm{NS}}$ or $\tau = \tau^{\mathrm{LS}}$. Although the discrete solution u_h depends on the choice of τ, this dependence will not be indicated by an additional index on u_h. The same applies to the mixed scheme below. The following result states the error analysis.

PROPOSITION 3.1. *Problem* (19) *is uniquely solvable. The error* $u - u_h$ *for the solution* $u \in V$ *to* (12) *and the discrete solution* $u_h \in V_h$ *to* (19) *satisfies*

$$\|D^2(u - u_h)\|_{L^2(\Omega)} \leq c(\gamma, \varepsilon)^{-1} \|A\|_{L^\infty(\Omega)} \inf_{v_h \in V_h} \|D^2(u - v_h)\|_{L^2(\Omega)}.$$

Globally, the following reliable a posteriori error estimate holds:

$$c(\gamma, \varepsilon)\|D^2(u - u_h)\|_{L^2(\Omega)} \leq \|A : D^2 u_h - f\|_{L^2(\Omega)}.$$

Furthermore, for any open subdomain $\omega \subseteq \Omega$*, the following local efficiency is valid:*

$$\|A : D^2 u_h - f\|_{L^2(\omega)} \leq \|A\|_{L^\infty(\omega)} \|D^2(u - u_h)\|_{L^2(\omega)}.$$

Proof. For $\tau = \tau^{\mathrm{NS}}$, the a priori result follows from combining Céa's lemma [3] with the lower bound (10). For $\tau = \tau^{\mathrm{LS}}$, it follows with (13) and similar arguments. Therein, the symmetry of the formulation allows the use of equivalence of norms, which implies the stated constant while a general Céa-type estimate would result in the square of that constant. The reliability result follows from the lower bound (10) and (9) for $\tau = \tau^{\mathrm{NS}}$ and $\tau = \tau^{\mathrm{LS}}$, respectively, and the fact that $f = D^2 u$ in the L^2 sense. The latter fact also proves the efficiency estimate. ∎

Several instances of finite-dimensional piecewise polynomial conforming subspaces V_h are known [5]. In the numerical experiments of section 5, the performance of the Bogner–Fox–Schmit (BFS) finite element under adaptive mesh-refinement based on the a posteriori error estimator of Proposition (3.1) is empirically studied.

3.2. Mixed discretization. The conformity assumption $V_h \subseteq H^2(\Omega)$ requires C^1 continuity and results in rather complicated local constructions. An alternative discretization is based on the formulation (16) and mixed Stokes-type finite elements [11]. Suppose that $W_h \subseteq W$ and $Q_h \subseteq Q$ are closed subspaces that satisfy for some positive constant $\tilde{\beta}$ that

$$\tilde{\beta} \leq \inf_{q_h \in Q_h \setminus \{0\}} \sup_{v_h \in W_h \setminus \{0\}} b(v_h, q_h) / (\|Dv_h\|_{L^2(\Omega)} \|q_h\|_{L^2(\Omega)}). \tag{20}$$

Since, in general, the property $b(v_h, q_h) = 0$ for all $q_h \in Q_h$ does not imply that $\operatorname{rot} v_h = 0$, the argument (8) is not applicable and coercivity of a on the kernel of b requires stabilization. The proposed stabilization is as follows. Define the constant

$$c_\lambda^\tau(\gamma, \varepsilon) := \begin{cases} \sqrt{1 - \frac{\lambda^2 + 1 - \varepsilon}{2\lambda}} & \text{if } \tau = \tau^{\mathrm{NS}}, \\ \frac{1 - \sqrt{1-\varepsilon}}{\|\gamma\|_{L^\infty(\Omega)}\sqrt{1+\lambda}} = c(\gamma, \varepsilon)/\sqrt{1+\lambda} & \text{if } \tau = \tau^{\mathrm{LS}} \end{cases}$$

for a given parameter $\lambda > 0$ which in the case $\tau = \tau^{\mathrm{NS}}$ is subject to the additional constraint $|\lambda - 1| < \sqrt{\varepsilon}$. It should also be noted that in the case $\tau = \tau^{\mathrm{NS}}$ the constant $c_\lambda^\tau(\gamma, \varepsilon)$ is independent of γ. The notation, however, is maintained for the sake of a unified presentation. Define furthermore the stabilization parameter

$$\sigma_\lambda^\tau(\gamma,\varepsilon) := \begin{cases} \sqrt{c_\lambda^\tau(\gamma,\varepsilon)^2 + (1-\varepsilon)/(2\lambda)} = \sqrt{1-\lambda/2} & \text{if } \tau = \tau^{\mathrm{NS}}, \\ \sqrt{c_\lambda^\tau(\gamma,\varepsilon)^2 + \frac{(1+1/\lambda)(1-\varepsilon)}{(1+\lambda)\|\gamma\|_{L^\infty(\Omega)}^2}} & \text{if } \tau = \tau^{\mathrm{LS}}. \end{cases}$$

Define the enriched bilinear form $\tilde{a}_\tau$ for any $v, z \in W$ through

$$\tilde{a}_\tau(v,z) := a_\tau(v,z) + \sigma_\lambda^\tau(\gamma,\varepsilon)^2(\operatorname{rot} v, \operatorname{rot} z)_{L^2(\Omega)}.$$

Let $S_h \subseteq H_0^1(\Omega)$ be a closed subspace. The discrete mixed system seeks $(u_h, w_h, p_h) \in S_h \times W_h \times Q_h$ such that

$$(\nabla u_h - w_h, \nabla z_h)_{L^2(\Omega)} = 0 \qquad \text{for all } z_h \in S_h, \tag{21a}$$

$$\tilde{a}_\tau(w_h, v_h) + b(v_h, p_h) = (f, \tau(v_h))_{L^2(\Omega)} \qquad \text{for all } v_h \in W_h, \tag{21b}$$

$$b(w_h, q_h) = 0 \qquad \text{for all } q_h \in Q_h. \tag{21c}$$

The following proposition states well-posedness and error estimates for (21) in the case $\tau = \tau^{\mathrm{NS}}$.

PROPOSITION 3.2. *Let $\tau = \tau^{\mathrm{NS}}$. For any $\lambda > 0$ such that $|\lambda - 1| \le \sqrt{\varepsilon}$, problem* (21) *admits a unique solution $(u_h, w_h, p_h) \in S_h \times W_h \times Q_h$. It satisfies the error estimate*

$$\|D^2 u - D w_h\|_{L^2(\Omega)} \le C(\lambda,\gamma,\varepsilon,\tau) \inf_{v_h \in W_h} \|D^2 u - D v_h\|_{L^2(\Omega)},$$

where $C(\lambda,\gamma,\varepsilon,\tau) = 4c_\lambda^\tau(\gamma,\varepsilon)^{-2}\tilde{\beta}^{-1}(\|\gamma\|_{L^\infty(\Omega)}\|A\|_{L^\infty(\Omega)} + \sigma_\lambda^\tau(\gamma,\varepsilon)^2)$. Moreover the following reliable a posteriori error estimate holds for any $\mu > 0$ with $\mu\|\gamma\|_{L^\infty(\Omega)}^2 \le 2c_\lambda^\tau(\gamma,\varepsilon)^2$,

$$\begin{aligned} &\sqrt{c_\lambda^\tau(\gamma,\varepsilon)^2 - 2^{-1}\mu\|\gamma\|_{L^\infty(\Omega)}^2}\|D^2 u - D w_h\|_{L^2(\Omega)} \\ &\qquad \le \sqrt{(2\mu)^{-1}\|A : D w_h - f\|_{L^2(\Omega)}^2 + \sigma_\lambda^\tau(\gamma,\varepsilon)^2\|\operatorname{rot} w_h\|_{L^2(\Omega)}^2}. \end{aligned}$$

For any open subdomain $\omega \subseteq \Omega$ we have the efficiency

$$\begin{aligned} &\sqrt{(2\mu)^{-1}\|A : D w_h - f\|_{L^2(\omega)}^2 + \sigma_\lambda^\tau(\gamma,\varepsilon)^2\|\operatorname{rot} w_h\|_{L^2(\omega)}^2} \\ &\qquad \le \sqrt{(2\mu)^{-1}\|A\|_{L^\infty(\omega)}^2 + \sigma_\lambda^\tau(\gamma,\varepsilon)^2}\|D^2 u - D w_h\|_{L^2(\omega)}. \end{aligned}$$

Proof. Let $v \in W$. The argument from the first line of (10) together with Lemma 2.1 and (8) leads to

$$\begin{aligned} &(A : Dv, \gamma \operatorname{div} v)_{L^2(\Omega)} \\ &\quad = \|\operatorname{div} v\|_{L^2(\Omega)}^2 + ((\gamma A - I_{d\times d}) : Dv, \operatorname{div} v)_{L^2(\Omega)} \\ &\quad \ge \|\operatorname{div} v\|_{L^2(\Omega)}^2 - \sqrt{1-\varepsilon}\|\operatorname{div} v\|_{L^2(\Omega)}\sqrt{\|\operatorname{div} v\|_{L^2(\Omega)}^2 + \|\operatorname{rot} v\|_{L^2(\Omega)}^2}. \end{aligned}$$

For any $\lambda > 0$, the Young inequality bounds the right-hand side from below by

$$\big(1 - \lambda/2 - (1-\varepsilon)/(2\lambda)\big)\|\operatorname{div} v\|^2_{L^2(\Omega)} - (1-\varepsilon)/(2\lambda)\|\operatorname{rot} v\|^2_{L^2(\Omega)}.$$

Elementary calculations with the foregoing two displayed expressions therefore lead, after adding $c^\tau_\lambda(\gamma,\varepsilon)^2\|\operatorname{rot} v\|^2_{L^2(\Omega)}$, to the coercivity

$$c^\tau_\lambda(\gamma,\varepsilon)^2\|Dv\|^2_{L^2(\Omega)} \le \tilde a_\tau(v,v) \quad \text{for any } v \in W. \tag{22}$$

The constant $c^\tau_\lambda(\gamma,\varepsilon)^2$ is positive if and only if $|\lambda - 1| < \sqrt{\varepsilon}$. This and (20) yield well-posedness. The a priori error estimate follows from the mixed finite element theory [2]; see [2, Thm. 5.2.2] for the precise constant. In particular, the best-approximation error of p does not appear in the error bound because that term equals zero due to $p = 0$. The proof of the reliability estimate employs the coercivity (22), the L^2 identity $A : D^2u = f$, as well as the Cauchy and Young inequalities with an arbitrary parameter $\mu > 0$,

$$\begin{aligned} &c^\tau_\lambda(\gamma,\varepsilon)^2\|D(\nabla u - w_h)\|^2_{L^2(\Omega)} \\ &\quad\le \tilde a_\tau(\nabla u - w_h, \nabla u - w_h) \le (2\mu)^{-1}\|A : Dw_h - f\|^2_{L^2(\Omega)} \\ &\qquad + 2^{-1}\mu\|\gamma\|^2_{L^\infty(\Omega)}\|D(\nabla u - w_h)\|^2_{L^2(\Omega)} + \sigma^\tau_\lambda(\gamma,\varepsilon)^2\|\operatorname{rot} w_h\|^2_{L^2(\Omega)}. \end{aligned}$$

This implies the stated reliability. The efficiency follows from $A : D^2u = f$ in L^2. ∎

The following proposition states well-posedness and error estimates for (21) in the case $\tau = \tau^{\mathrm{LS}}$.

PROPOSITION 3.3. *Let $\tau = \tau^{\mathrm{LS}}$. For any $\lambda > 0$, problem (21) admits a unique solution $(u_h, w_h, p_h) \in S_h \times W_h \times Q_h$. It satisfies the error estimate*

$$\|D^2u - Dw_h\|_{L^2(\Omega)} \le C(\lambda,\gamma,\varepsilon,\tau) \inf_{v_h \in W_h} \|D^2u - Dv_h\|_{L^2(\Omega)},$$

where

$$C(\lambda,\gamma,\varepsilon,\tau) = 2\frac{\sqrt{\|A\|^2_{L^\infty(\Omega)} + \sigma^\tau_\lambda(\gamma,\varepsilon)^2}}{c^\tau_\lambda(\gamma,\varepsilon)}\left[\tilde\beta^{-1} + \frac{\sqrt{\|A\|^2_{L^\infty(\Omega)} + \sigma^\tau_\lambda(\gamma,\varepsilon)^2}}{c^\tau_\lambda(\gamma,\varepsilon)}\right].$$

Moreover the following reliable a posteriori error estimate holds:

$$c^\tau_\lambda(\gamma,\varepsilon)\|D^2u - Dw_h\|_{L^2(\Omega)} \le \sqrt{\|A : Dw_h - f\|^2_{L^2(\Omega)} + \sigma^\tau_\lambda(\gamma,\varepsilon)^2\|\operatorname{rot} w_h\|^2_{L^2(\Omega)}}.$$

For any open subdomain $\omega \subseteq \Omega$ we have the efficiency

$$\begin{aligned} &\sqrt{\|A : Dw_h - f\|^2_{L^2(\omega)} + \sigma^\tau_\lambda(\gamma,\varepsilon)^2\|\operatorname{rot} w_h\|^2_{L^2(\omega)}} \\ &\qquad\qquad \le \sqrt{\|A\|^2_{L^\infty(\omega)} + \sigma^\tau_\lambda(\gamma,\varepsilon)^2}\|D^2u - Dw_h\|_{L^2(\omega)}. \end{aligned}$$

Proof. The estimate (6) and Lemma 2.1, the relation (8), and the triangle inequality prove for any $v \in W$ that

$$\begin{aligned} \|\operatorname{div} v\|_{L^2(\Omega)} &\le \|\gamma A : Dv\|_{L^2(\Omega)} + \sqrt{1-\varepsilon}\|Dv\|_{L^2(\Omega)} \\ &\le \|\gamma\|_{L^\infty(\Omega)}\|A : Dv\|_{L^2(\Omega)} + \sqrt{1-\varepsilon}\,(\|\operatorname{div} v\|_{L^2(\Omega)} + \|\operatorname{rot} v\|_{L^2(\Omega)}). \end{aligned}$$

With the constant $c(\gamma,\varepsilon)$, this is equivalent to

$$c(\gamma,\varepsilon)\|\operatorname{div} v\|_{L^2(\Omega)} \le \|A:Dv\|_{L^2(\Omega)} + \sqrt{1-\varepsilon}/\|\gamma\|_{L^\infty(\Omega)}\|\operatorname{rot} v\|_{L^2(\Omega)}.$$

Taking squares on both sides and using the Young inequality, one arrives at

$$\begin{aligned} &c(\gamma,\varepsilon)^2\|\operatorname{div} v\|^2_{L^2(\Omega)} \\ &\quad\le (1+\lambda)\|A:Dv\|^2_{L^2(\Omega)} + (1+1/\lambda)(1-\varepsilon)/\|\gamma\|^2_{L^\infty(\Omega)}\|\operatorname{rot} v\|^2_{L^2(\Omega)}. \end{aligned}$$

Adding $c(\gamma,\varepsilon)^2\|\operatorname{rot} v\|^2_{L^2(\Omega)}$ and dividing by $(1+\lambda)$ leads with (8) to

$$c^\tau_\lambda(\gamma,\varepsilon)^2\|Dv\|^2_{L^2(\Omega)} \le \|A:Dv\|^2_{L^2(\Omega)} + \sigma^\tau_\lambda(\gamma,\varepsilon)^2\|\operatorname{rot} v\|^2_{L^2(\Omega)}.$$

Hence, $\tilde a$ satisfies the coercivity

$$c^\tau_\lambda(\gamma,\varepsilon)^2\|Dv\|^2_{L^2(\Omega)} \le \tilde a(v,v) \quad \text{for any } v\in W.$$

As in the proof of Proposition 3.2, this and the stability condition (20) establish the unique solvability and the a priori error estimate with the constant from [2, Thm. 5.2.2]. The proof of the a posteriori bounds is immediate. ∎

Remark 3. The a posteriori bounds in Propositions 3.1, 3.2, 3.3 are fully explicit. The evaluation of integrals of the L^∞ coefficient A may, however, be computationally challenging in practice; cf. the numerical experiments in section 5.

Remark 4. Clearly, an a priori error estimate for the difference $p-p_h$ in the L^2 norm in the fashion of Propositions 3.2, 3.3 can also be obtained. Since, in this context, the Lagrange multiplier is not of particular interest, its analysis not included in the proposition. Moreover, using (20) and the fact that $p=0$, it can be shown that the error is bounded from above by some constant times the suggested error estimator.

Remark 5. In three space dimensions, subspaces of Q must satisfy a pointwise divergence-free constraint. In [11] the space Q_h of divergence-free lowest-order Raviart–Thomas fields was used. This space Q_h consists exactly of all piecewise constant vector fields that are continuous in the inter-element normal directions and whose normal component vanishes on the boundary $\partial\Omega$. Another approach could be to further soften the formulation by enforcing the divergence-free constraint in a weak manner. This would involve an additional Lagrange multiplier also arising in the error estimates.

4. An adaptive algorithm and its convergence. This section is devoted to the description of an adaptive algorithm for the discretization methods from section 3 and the proof of its convergence.

4.1. Assumptions on the discrete spaces. Let $\mathbb{T}$ denote a set of admissible shape-regular partitions refined from some initial mesh $\mathcal{T}_0$ of $\overline{\Omega}$. The partitions may consist of triangles/tetrahedra or quadrilaterals/hexahedra. Shape-regularity is meant in the sense that (i) there exist positive constants c and C such that for any $\mathcal{T}\in\mathbb{T}$ and any $T\in\mathcal{T}$, $c\operatorname{meas}(T) \le \operatorname{diam}(T)^d \le C\operatorname{meas}(T)$ and (ii) any two neighboring elements $T,K\in\mathcal{T}$ satisfy $c\le \operatorname{diam}(T)/\operatorname{diam}(K)$. This property is respected by many refinement routines like newest-vertex bisection [1], but also refinements involving hanging nodes are allowed as long as the number of hanging nodes per interface stays uniformly bounded. The shape-regularity implies that there is some $\alpha>0$ such

that any $T \in \mathcal{T} \in \mathbb{T}$ and any refined element $\hat{T} \subsetneq T$ in a refined partition $\widehat{\mathcal{T}}$ satisfy $\operatorname{meas}(\hat{T}) \leq \alpha \operatorname{meas}(T)$. The discretization spaces from section 3.1 (resp., section 3.2) are labelled with the partitions in $\mathbb{T}$ and are denoted by $V(\mathcal{T})$ (resp., $W(\mathcal{T})$ and $Q(\mathcal{T})$) rather than V_h, etc., in section 3. The spaces are assumed to be nested on refined triangulations. It is assumed that $\mathbb{T}$ contains sufficiently many refinements so that for any $\mathcal{T} \in \mathbb{T}$ and any $\delta > 0$ there is some refinement $\widehat{\mathcal{T}} \in \mathbb{T}$ such that for any $T \in \widehat{\mathcal{T}}$ the diameter satisfies $\operatorname{diam}(T) \leq \delta$. It is furthermore assumed that there exist a stable, projective, quasi-local quasi-interpolation operator, i.e., there is a constant C such that for any $\mathcal{T} \in \mathbb{T}$ there is a linear idempotent map $I_{\mathcal{T}} : V \to V(\mathcal{T})$ (resp., $I_{\mathcal{T}} : W \to W(\mathcal{T})$ for the mixed method) such that, for any $T \in \mathcal{T}$, the estimate

(23)
$$\|D^2 I_{\mathcal{T}} v\|_{L^2(T)} \leq C \|D^2 v\|_{L^2(\omega_T)} \quad \text{for any } v \in V$$
$$\text{(resp., } \operatorname{diam}(T)^{-1} \|z - I_{\mathcal{T}} z\|_{L^2(T)} + \|D I_{\mathcal{T}} z\|_{L^2(T)} \leq C \|Dz\|_{L^2(\omega_T)} \text{ for any } z \in W)$$

holds, where ω_T denotes the element-patch of T, i.e., the union of all elements of $\mathcal{T}$ sharing a point with T. (This assumption can be relaxed by requiring ω_T to be some surrounding domain with finite overlap property.) Since this quasi-interpolation is a stable projection, it is also quasi-optimal. It is assumed that for any sequence $(\mathcal{T}_\ell)_\ell$ of partitions with $\max_{T \in \mathcal{T}_\ell} \operatorname{diam}(T) \to 0$ as $\ell \to \infty$, the spaces $V(\mathcal{T}_\ell)$ (resp., $W(\mathcal{T}_\ell)$) are dense in V (resp., W). This implies that, for any $v \in V$, the quasi-interpolation $I_{\mathcal{T}_\ell} v$ converges to v in the H^2 norm (resp., in the H^1 norm). These requirements are met for most of the known H^2 conforming finite elements based on piecewise polynomials. It is, however, important to note that not all H^2 conforming finite elements lead to nested spaces. The Argyris FEM and the Hsieh–Clough–Tocher FEM [5], for example, do not satisfy this property. A positive example is the BFS FEM [5] used in the numerical experiments below. In the case of mixed methods, the discretizations of W need only be H^1 conforming, and quasi-interpolation operators for such spaces are well-established. Their existence is typically assured through the shape-regularity. In addition, the mixed finite element spaces are assumed to satisfy Assumption 1 stated below.

4.2. Adaptive algorithm and convergence proof. The algorithm departs from an initial mesh $\mathcal{T}_0$ and runs the following loop over the index $\ell = 0, 1, 2, \ldots$.

Solve. Solve the discrete problem (19) (resp., (21)) with respect to the mesh $\mathcal{T}_\ell$ and the space $V(\mathcal{T}_\ell)$. Denote the solution by u_ℓ (resp., (w_ℓ, p_ℓ)).

Estimate. Compute, for any $T \in \mathcal{T}_\ell$, the local error estimator contributions $\eta_\ell^2(T) = \|A : D^2 u_\ell - f\|_{L^2(T)}^2$ (resp., $\eta_\ell^2(T) = \|A : Dw_\ell - f\|_{L^2(T)}^2 + \sigma_\lambda^\tau(\gamma, \varepsilon)^2 \|\operatorname{rot} w_\ell\|_{L^2(T)}^2$).

Mark. Choose some (any) subset $\mathcal{M}_\ell \subseteq \mathcal{T}_\ell$ satisfying $T \in \mathcal{M}_\ell$ for at least one $T \in \mathcal{T}_\ell$ with $\eta_\ell^2(T) = \max_{K \in \mathcal{T}_\ell} \eta_\ell^2(K)$.

Refine. Compute a refined admissible partition $\mathcal{T}_{\ell+1}$ of $\mathcal{T}_\ell$ such that at least all elements of $\mathcal{M}_\ell$ are refined.

Remark 6. In view of the different weights in the error estimators of Propositions 3.2–3.3, it is worth mentioning that one can choose different weights for the contributions of $\eta_\ell(T)$. This is, however, of minor importance for the convergence analysis.

This adaptive algorithm is formulated in a fairly general way (see also [17]); it admits various existing marking procedures, for instance, the maximum marking or the Dörfler marking [8]. The refinement step typically involves some minimality condi-

tion on the refined partition to gain efficiency. In section 5 an instance of an adaptive algorithm with more details is presented. However, the present form of the algorithm suffices for convergence. A similar argument was used by [17]. The difference is that the residuals in the present error estimator are strong L^2 residuals. This has the effect that no data oscillations enter the convergence analysis. The main reason is that the efficiency proof does not require the usual techniques employing bubble functions [24].

Consider the sequence $(\mathcal{T}_\ell)_\ell$ produced by the adaptive algorithm. The convergence proofs employ the subset $\mathcal{K} \subseteq \cup_{\ell\geq 0}\mathcal{T}_\ell$ of never refined elements defined by

$$\mathcal{K} := \bigcup_{\ell\geq 0}\bigcap_{m\geq \ell} \mathcal{T}_m.$$

The set was already utilized in [17]. It is the set of elements that are never refined once they are created. Accordingly, for any $\ell \geq 0$, the partition $\mathcal{T}_\ell$ can be written as the following disjoint union

$$\mathcal{T}_\ell = \mathcal{K}_\ell \cup \mathcal{R}_\ell \qquad \text{for } \mathcal{K}_\ell := \mathcal{K} \cap \mathcal{T}_\ell \text{ and } \mathcal{R}_\ell := \mathcal{T}_\ell \setminus \mathcal{K}_\ell. \tag{24}$$

By definition, every element of $\mathcal{R}_\ell$ is eventually refined and the measure of those children that do not belong to $\mathcal{K}$ is reduced by a factor α. Hence, for any $\varepsilon > 0$ there exists some $\ell_0 \geq 0$ such that, for all $\ell \geq \ell_0$,

$$\max_{T\in\mathcal{R}_\ell} \operatorname{meas}(T) < \varepsilon. \tag{25}$$

The following result proves the convergence of the adaptive conforming scheme. More details on the arguments employed here can be found in, e.g., [17, 18].

PROPOSITION 4.1. *Let $\tau = \tau^{\mathrm{NS}}$ or $\tau = \tau^{\mathrm{LS}}$. Let the admissible partitions $\mathbb{T}$ and the discrete spaces $V(\mathcal{T})$ for any $\mathcal{T} \in \mathbb{T}$ satisfy the assumptions from the beginning of this section. Then the sequence $u_\ell \in V(\mathcal{T}_\ell)$ produced by the adaptive algorithm converges to the exact solution $u \in V$, i.e., $\|D^2(u - u_\ell)\|_{L^2(\Omega)} \to 0$ as $\ell \to \infty$.*

Proof. The sequence $(u_\ell)_\ell$ converges in V to some limit $u_\star$ (because the u_ℓ are in particular the Galerkin approximations of the variational problem posed on the closure of the union of the nested spaces $V(\mathcal{T}_\ell)$, $\ell \geq 0$), i.e.,

$$\|D^2(u_\star - u_\ell)\|_{L^2(\Omega)} \to 0 \quad \text{as } \ell \to \infty.$$

It is not a priori known that $u_\star = u$, since it is not clear whether the global mesh-size converges to zero in all regions of the domain Ω. Recall decomposition (24) of $\mathcal{T}_\ell$ in never refined ($\mathcal{K}_\ell$) and eventually refined ($\mathcal{R}_\ell$) elements. The local efficiency of the error estimator (Proposition 3.1) and the triangle inequality prove for any $T \in \mathcal{T}_\ell$ that

$$\eta_\ell^2(T) \leq 2\|A\|^2_{L^\infty(\Omega)}\big(\|D^2(u - u_\star)\|^2_{L^2(T)} + \|D^2(u_\star - u_\ell)\|^2_{L^2(T)}\big).$$

Since $\|D^2(u_\star - u_\ell)\|_{L^2(T)} \to 0$ as $\ell \to \infty$, one concludes with (25) that for any $\rho > 0$ there exists some $\tilde{\ell}_0 \geq 0$ such that, for all $\ell \geq \tilde{\ell}_0$,

$$\max_{T\in\mathcal{K}_\ell} \eta_\ell^2(T) \leq \max_{T\in\mathcal{R}_\ell} \eta_\ell^2(T) < \rho.$$

(If this was not the case, the properties of the marking step would imply that eventually an element in $\mathcal{K}_\ell$ is refined, which contradicts its membership in $\mathcal{K}_\ell$.) In

conclusion, for any $T \in \mathcal{K}$, $\|A : D^2 u_\ell - f\|_{L^2(T)} \to 0$ as $\ell \to \infty$. In order to conclude convergence in $L^2(\cup\mathcal{K})$, observe that $\sum_{T\in\mathcal{K}} \operatorname{meas}(T) \leq \operatorname{meas}(\Omega)$, that is, the series on the left-hand side converges. Thus, the measure of $(\cup\mathcal{K}) \setminus (\cup\mathcal{K}_m)$ becomes arbitrary small for sufficiently large m. Given $\delta > 0$, the dominated convergence theorem therefore implies that, for sufficiently large m_0 and all $m \geq m_0$, $\|A : D^2 u_\star - f\|_{L^2((\cup\mathcal{K})\setminus(\cup\mathcal{K}_m)))} \leq \delta/2$. The elementwise convergence and $u_\ell \to u_\star$ in $H^2(\Omega)$ therefore imply that, for some sufficiently large $\hat{\ell}_0 > 0$, it holds that

$$\begin{aligned}
&\|A : D^2 u_\ell - f\|_{L^2(\cup\mathcal{K})} \\
&\quad \leq \|A : D^2 u_\ell - f\|_{L^2(\cup\mathcal{K}_{m_0})} + \|A : D^2(u_\ell - u_\star)\|_{L^2((\cup\mathcal{K})\setminus(\cup\mathcal{K}_{m_0}))} \\
&\qquad + \|A : D^2 u_\star - f\|_{L^2((\cup\mathcal{K})\setminus(\cup\mathcal{K}_{m_0}))} \leq \delta \qquad \text{for all } \ell \geq \hat{\ell}_0.
\end{aligned}$$

Hence, $\|A : D^2 u_\ell - f\|_{L^2(\cup\mathcal{K})} \to 0$ as $\ell \to \infty$.

The L^2 identity $A : D^2 u = f$, the definition of τ and (10) imply

$$\sum_{T\in\mathcal{T}_\ell} \eta_\ell^2(T) \begin{cases} \leq \frac{\|A\|^2_{L^\infty(\Omega)}}{1-\sqrt{1-\varepsilon}} (A : D^2(u-u_\ell), \tau(\nabla(u-u_\ell)))_{L^2(\Omega)} & \text{if } \tau = \tau^{\mathrm{NS}}, \\ = (A : D^2(u-u_\ell), \tau(\nabla(u-u_\ell)))_{L^2(\Omega)} & \text{if } \tau = \tau^{\mathrm{LS}}. \end{cases}$$

Thus, with a constant $c > 0$ (depending on the choice of τ), the Galerkin orthogonality, the Cauchy inequality, and the L^2 identity $A : D^2 u = f$ lead, for any $\ell \geq 0$, to

$$\begin{aligned}
c \sum_{T\in\mathcal{T}_\ell} \eta_\ell^2(T) &\leq (A : D^2(u-u_\ell), \tau(\nabla(u-u_\ell)))_{L^2(\Omega)} \\
&= (A : D^2(u-u_\ell), \tau(\nabla(u-I_{\mathcal{T}_\ell} u)))_{L^2(\Omega)} \\
&\leq \|A : D^2 u_\ell - f\|_{L^2(\cup\mathcal{K})} \|\tau(\nabla(u-I_{\mathcal{T}_\ell} u))\|_{L^2(\cup\mathcal{K})} \\
&\quad + \|A : D^2 u_\ell - f\|_{L^2(\cup\mathcal{R}_\ell)} \|\tau(\nabla(u-I_{\mathcal{T}_\ell} u))\|_{L^2(\cup\mathcal{R}_\ell)}.
\end{aligned}$$

The convergence $A : D^2 u_\ell \to f$ in $L^2(\cup\mathcal{K})$ and the convergence of the quasi-interpolation show that both summands on the right-hand side converge to zero. Since by Proposition 3.1 the error estimator is reliable, the proof is concluded. ∎

The convergence proof of the mixed scheme requires a mild structural hypothesis on the discrete spaces. Let $\ell \in \mathbb{N}$ and $T \in \mathcal{K}_\ell$ and consider the first-order neighborhood and its triangulation defined by

$$\omega_{T,\mathcal{K}} := \operatorname{int}(\cup\{K \in \mathcal{K} : T \cap K \neq \emptyset\}) \quad \text{with} \quad \mathcal{T}(\omega_{T,\mathcal{K}}) := \{K \in \mathcal{K} : T \cap K \neq \emptyset\}.$$

The shape-regularity assumption assures that there exists $n(\ell, T) \geq \ell$ such that $\mathcal{T}(\omega_{T,\mathcal{K}}) \subseteq \mathcal{K}_m$ holds for all $m \geq n(\ell, T)$. This means that, eventually, all neighbors of T belong to $\mathcal{K}$. Define the spaces $W(\mathcal{T}(\omega_{T,\mathcal{K}}))$ of functions in $W(\mathcal{T}_m)$ with support in $\overline{\omega_{T,\mathcal{K}}}$ and $Q(\mathcal{T}(\omega_{T,\mathcal{K}}))$ of functions from $Q(\mathcal{T}_m)$ that are restricted to $\omega_{T,\mathcal{K}}$.

Assumption 1. All $\ell \in \mathbb{N}$ and all $T \in \mathcal{K}_\ell$ satisfy the following: if $q \in Q(\mathcal{T}(\omega_{T,\mathcal{K}}))$ fulfils $(\operatorname{rot} v, q)_{L^2(\omega_{T,\mathcal{K}})} = 0$ for all $v \in W(\mathcal{T}(\omega_{T,\mathcal{K}}))$, then $(\operatorname{rot} v, q)_{L^2(\omega_{T,\mathcal{K}})} = 0$ holds for all $v \in H^1_0(\omega_{T,\mathcal{K}}; \mathbb{R}^d)$.

Assumption 1 basically states that a full-rank condition like (20) remains true on element patches. It is, however, a purely algebraic and thus weaker condition. As will turn out in the proof of Proposition 4.2, the assumption could be further relaxed by allowing other suitable overlapping neighborhoods. In two space dimensions, Assumption 1 (or a relaxed version with larger patches) is satisfied by many (if not all) known

finite elements for the Stokes problem. In particular, pairings whose stability proof is based on the design of a Fortin operator or the macroelement technique are included. Pathological situations in which an element T does not have enough neighbors (e.g., all vertices on lie on $\partial\mathcal{K}$) can only occur if T meets the boundary $\partial\Omega$ (due to the shape-regularity). Hence, such situations are excluded if the class $\mathbb{T}$ of triangulations is chosen properly. In three dimensions, where the problem significantly differs from the Stokes equations, the pairing from [11], which is based on face-bubble stabilization, satisfies Assumption 1. In all these cases, the verification of Assumption 1 is independent of any a priori knowledge about the sets $\mathcal{K}_\ell$. The next result proves the convergence of the adaptive mixed scheme.

PROPOSITION 4.2. *Let $\tau = \tau^{\mathrm{NS}}$ or $\tau = \tau^{\mathrm{LS}}$. Let the admissible partitions $\mathbb{T}$ and the discrete spaces $W(\mathcal{T})$, $Q(\mathcal{T})$ for any $\mathcal{T} \in \mathbb{T}$ satisfy the assumptions from the beginning of this section as well as Assumption 1. Then the sequence $(w_\ell, p_\ell) \in W(\mathcal{T}_\ell) \times Q(\mathcal{T}_\ell)$ produced by the adaptive algorithm converges to the exact solution $(w,p) \in W \times Q$. In particular, $\|D^2 u - Dw_\ell\|_{L^2(\Omega)} \to 0$ as $\ell \to \infty$.*

Proof. Similarly as in the proof of Proposition 4.1, one can show that there exists a limit $(w_\star, p_\star) \in W \times Q$ such that $\|D(w_\star - w_\ell)\|_{L^2(\Omega)} + \|p_\star - p_\ell\|_{L^2(\Omega)} \to 0 \quad \text{as } \ell \to \infty$. Consider again the set $\mathcal{K}$ and the decomposition (24). The local efficiency of the error estimator (Propositions 3.2 and 3.3) and the triangle inequality prove for some constant $C > 0$ (depending on the choice of τ) and any $T \in \mathcal{T}_\ell$ that

$$\eta_\ell^2(T) \le C\big(\|D(w - w_\star)\|_{L^2(T)}^2 + \|D(w_\star - w_\ell)\|_{L^2(T)}^2\big).$$

As in the proof of Proposition 4.1, one obtains

$$\|A : Dw_\ell - f\|_{L^2(\cup\mathcal{K})} + \|\operatorname{rot} w_\ell\|_{L^2(\cup\mathcal{K})} \to 0 \quad \text{as } \ell \to \infty.$$

Similarly as in the proof of Proposition 4.1, the coercivity of $\tilde{a}_\tau$ shows that there exists a constant $c > 0$ (depending on the choice of τ) such that with the L^2 identity $A : Dw = f$ and the quasi-interpolation $I_{\mathcal{T}_\ell}$ the following split is valid:

$$\begin{aligned} c \sum_{T \in \mathcal{T}_\ell} \eta_\ell^2(T) &\le (A : D(w - w_\ell), \tau(w - I_{\mathcal{T}_\ell} w))_{L^2(\Omega)} \\ &\quad + (A : D(w - w_\ell), \tau(I_{\mathcal{T}_\ell} w - w_\ell))_{L^2(\Omega)} + \sigma_\lambda^\tau(\gamma,\varepsilon)^2 \|\operatorname{rot} w_\ell\|_{L^2(\Omega)}^2. \end{aligned} \tag{26}$$

The first term on the right-hand side of (26) can be shown to converge to zero with the techniques from Proposition 4.1 because locally it consists of products of error estimator and interpolation error contributions. Using the discrete equations (21b)–(21c) and $A : Dw = f$, the remaining terms of (26) are transformed into

$$\sigma_\lambda^\tau(\gamma,\varepsilon)^2 (\operatorname{rot} w_\ell, \operatorname{rot} I_{\mathcal{T}_\ell} w)_{L^2(\Omega)} + (\operatorname{rot} I_{\mathcal{T}_\ell} w, p_\ell)_{L^2(\cup\mathcal{R}_\ell)} + (\operatorname{rot} I_{\mathcal{T}_\ell} w, p_\ell)_{L^2(\cup\mathcal{K}_\ell)}. \tag{27}$$

Since $\operatorname{rot} I_{\mathcal{T}_\ell} w = \operatorname{rot}(I_{\mathcal{T}_\ell} w - w)$, the first and second term can again be shown to converge to zero: the first term is an elementwise product of error estimator and interpolation error contributions, while the second one is controlled by the interpolation error on the elements of $\mathcal{R}_\ell$. The last term of (27) can be rewritten as $(\operatorname{rot} I_{\mathcal{T}_\ell} w, p_\ell - p_\star)_{L^2(\cup\mathcal{K}_\ell)} + (\operatorname{rot} I_{\mathcal{T}_\ell} w, p_\star)_{L^2(\cup\mathcal{K}_\ell)}$ and, since $p_\ell \to p_\star$ in L^2, it remains to estimate the term $(\operatorname{rot} I_{\mathcal{T}_\ell} w, p_\star)_{L^2(\cup\mathcal{K}_\ell)}$.

For the analysis of this term, it is useful to note that, for any connected component $\tilde{\omega}$ of $\cup\mathcal{K} \setminus \partial(\cup\mathcal{K})$, the function $p_\star|_{\tilde{\omega}}$ satisfies $(\operatorname{rot} v, p_\star)_{L^2(\tilde{\omega})} = 0$ for all $v \in H_0^1(\Omega;\mathbb{R}^d)$

with support in $\tilde{\omega}$. For the proof of this claim, let $\omega \subseteq \cup\mathcal{K}_\ell \setminus \partial(\cup\mathcal{K}_\ell)$ be a connected component of $\cup\mathcal{K}_\ell \setminus \partial(\cup\mathcal{K}_\ell)$. It is not difficult to see that ω is an open subset of one of the connected components of $\cup\mathcal{K} \setminus \partial(\cup\mathcal{K})$. Let $\mathcal{K}_\ell(\omega)$ denote the set of all elements of $\mathcal{K}_\ell$ whose interior has a nonempty intersection with ω. It is easily verified that the limit $(w_\star, p_\star)$ satisfies $\tilde{a}_\tau(w_\star, v_\ell) + b(v_\ell, p_\star) = (f, \tau(v_\ell))_{L^2(\Omega)}$ for all $\ell \geq 0$ and all $v_\ell \in W(\mathcal{T}_\ell)$ supported in ω. The fact that $A : Dw_\star = f$ and $\operatorname{rot} w_\star = 0$ in the L^2 sense on $\cup\mathcal{K}$ show that $(\operatorname{rot} v_\ell, p_\star)_{L^2(\Omega)} = 0$. Assumption 1 and an overlap argument prove that $(\operatorname{rot} v, p_\star)_{L^2(\tilde{\omega})} = 0$ for any $v \in H^1_0(\tilde{\omega}; \mathbb{R}^d)$ with compact support inside $\tilde{\omega}$, which implies the claim.

Let $\mu \in W^{1,\infty}(\omega)$ denote a positive cutoff function with values in the interval $[0,1]$ taking the value 1 on all elements of $\mathcal{K}_\ell(\omega)$ that do not meet the boundary $\Gamma_\omega := \partial(\cup\mathcal{K}_\ell) \setminus \partial\Omega$, that vanishes on Γ_ω, and that satisfies, for some constant C and for any element $T \in \mathcal{K}_\ell(\omega)$ touching Γ that $\|\nabla\mu\|_{L^\infty(T)} \leq C \operatorname{diam}(T)^{-1}$. The boundary conditions of μ, the identity $\operatorname{rot} w = 0$, and the product rule lead to

$$
\begin{aligned}
&|(\operatorname{rot}(I_{\mathcal{T}_\ell} w), p_\star)_{L^2(\omega)}| \\
&\quad = |(\operatorname{rot}((1-\mu)(w - I_{\mathcal{T}_\ell} w)), p_\star)_{L^2(\omega)}| \\
&\quad \leq \sum_{\substack{T \in \mathcal{K}_\ell(\omega) \\ T \cap \Gamma_\omega \neq \emptyset}} \big(\|\operatorname{rot}(w - I_{\mathcal{T}_\ell} w)\|_{L^2(T)} + C \operatorname{diam}(T)^{-1} \|w - I_{\mathcal{T}_\ell} w\|_{L^2(T)} \big) \, \|p_\star\|_{L^2(T)}.
\end{aligned}
$$

Using the Cauchy inequality and (23), this term can be shown to converge to zero because by the shape-regularity the measure of the elements in $\mathcal{T}_\ell$ meeting the boundary $\partial(\cup\mathcal{K}_\ell) \setminus \partial\Omega$ converges to zero as $\ell \to \infty$. In conclusion, the error estimator converges to zero, and so does the error. ∎

5. Numerical results. This section presents numerical experiments in two space dimensions for the choice τ^{LS}, that is, the least-squares method.

5.1. Numerical realization. This subsection describes the employed finite element methods and the used adaptive algorithm.

5.1.1. Conforming scheme. The H^2-conforming method used here is the BFS finite element [5]. Let $\mathcal{T}$ be a rectangular partition of Ω, where one hanging node (that is a point shared by two or more rectangles which is not vertex to all of them) per edge is allowed. The finite element space V_h is the subspace of V consisting of piecewise bicubic polynomials. It is a second-order scheme with expected convergence of $\mathcal{O}(h^2)$ for H^4-regular solutions on quasi-uniform meshes with maximal mesh-size h. For the error in the H^1 and the L^2 norm, the corresponding convergence order is $\mathcal{O}(h^3)$ and $\mathcal{O}(h^4)$, respectively.

5.1.2. Mixed scheme. As a mixed scheme, the Taylor–Hood finite element [2] is used. For a regular triangulation of $\mathcal{T}$ of Ω, the space W_h is the subspace of W consisting of piecewise quadratic polynomials while Q_h is the subspace of Q consisting of piecewise affine and globally continuous functions. It is a second-order scheme with expected convergence of $\mathcal{O}(h^2)$ for H^3-regular solution w (meaning that u is H^4-regular) on quasi-uniform meshes. For the error $\|w - \nabla u_h\|_{L^2(\Omega)}$, the corresponding convergence order is $\mathcal{O}(h^3)$. The computation of the primal variable u_h is performed with a standard finite element method based on piecewise quadratics. The predicted convergence order in the L^2 norm is $\mathcal{O}(h^3)$.

5.1.3. Adaptive algorithm. For any element $T \in \mathcal{T}$ the error estimators of Propositions 3.1 and 3.3 are abbreviated as follows:

$$\eta^2_{\mathrm{conf}}(T) = \|A : D^2 u_h - f\|^2_{L^2(T)},$$
$$\eta^2_{\mathrm{mixed}}(T) = \|A : Dw_h - f\|^2_{L^2(T)} + \sigma^\tau_\lambda(\gamma,\varepsilon)^2 \|\operatorname{rot} w_h\|^2_{L^2(T)}.$$

Furthermore set $\eta_{\mathrm{conf}} := \sqrt{\sum_{T\in\mathcal{T}} \eta^2_{\mathrm{conf}}(T)}$, $\eta_{\mathrm{mixed}} := \sqrt{\sum_{T\in\mathcal{T}} \eta^2_{\mathrm{mixed}}(T)}$. The following adaptive algorithm is a concrete instance of the procedure outlined in section 4. It is based on the Dörfler marking [8] for some parameter $0 < \theta \le 1$. In the following, η_ℓ refers to η_{conf} or η_{mixed}, depending on the used method. Departing from an initial mesh $\mathcal{T}_0$ it runs the following loop over the index $\ell = 0, 1, 2, \ldots$.

Solve. Solve the discrete problem with respect to the mesh $\mathcal{T}_\ell$.

Estimate. Compute the local error estimator contributions $\eta^2_\ell(T)$, $T \in \mathcal{T}_\ell$, for the discrete solution.

Mark. Mark a minimal subset $\mathcal{M} \subseteq \mathcal{T}_\ell$ such that $\theta\eta^2_\ell \le \sum_{T\in\mathcal{M}} \eta^2_\ell(T)$.

Refine. Compute a refined admissible partition $\mathcal{T}_{\ell+1}$ of $\mathcal{T}_\ell$ of minimal cardinality such that all elements of $\mathcal{M}$ are refined.

For rectangular meshes, the local refinement splits every rectangle in four congruent subrectangles while further local refinements assure the property of only one hanging node per edge. On triangular meshes, newest-vertex bisection [1] is employed.

5.2. Setup. In all numerical experiments the domain is the square $\Omega = (-1,1)^2$. The parameter λ for the stabilization in the mixed scheme is chosen as $\lambda = 1$. All convergence history plots are logarithmically scaled. The errors are plotted against the number of degrees of freedom `ndof`, that is, the space dimension of V_h, respectively, of $W_h \times Q_h$. In the adaptive computation, the parameter θ is chosen $\theta = 0.3$. The coefficient A reads

$$A = \begin{bmatrix} 2 & x_1x_2/(|x_1|\,|x_2|) \\ x_1x_2/(|x_1|\,|x_2|) & 2 \end{bmatrix}.$$

The requirements of section 2 are met with $\varepsilon = 3/5$, $\|\gamma\|_{L^\infty(\Omega)} = 2/5$, and $\|A\|_{L^\infty(\Omega)} = 2$, so that $c(\gamma,\varepsilon) = 5/2 - \sqrt{5/2} > 0.91886$. Three test cases are considered.

5.3. Experiment 1. In the first experiment the known smooth solution $u(x) = x_1x_2(1 - \exp(1 - |x_1|)(1 - \exp(1 - |x_2|)$ from [21] is considered. The convergence history is displayed in Figure 1 for the conforming BFS discretization and in Figure 2 for the mixed Taylor–Hood method. The convergence rates are of optimal order, that is, $\mathcal{O}(\mathtt{ndof}^{-1})$ for the approximation of the Hessian and $\mathcal{O}(\mathtt{ndof}^{-3/2})$ for the approximation of the gradient. With the BFS element, u is approximated at the optimal rate $\mathcal{O}(\mathtt{ndof}^{-2})$. The mixed method gives the rate $\mathcal{O}(\mathtt{ndof}^{-3/2})$, which is optimal for the used quadratic FEM. Since the solution in this example is smooth and the discontinuities of the coefficient match with the initial meshes, uniform refinement leads to the same rates as adaptive refinement. In the case of a nonmatching initial triangulation, uniform mesh refinement leads to reduced convergence rates as shown in Figure 3, whereas the adaptive BFS and Taylor–Hood schemes seem to behave optimally. The initial rectangular mesh is the square subdivided in four rectangles meeting at $(0.1, 0.2)$. The initial triangular mesh is created by inserting a "criss" diagonal in each of those four rectangles. A more challenging example is given below.

5.4. Experiment 2. The known singular solution reads in polar coordinates as

$$u(r,\theta) = \begin{cases} r^{5/3}(1-r)^{5/2}\sin(2\theta/3)^{5/2} & \text{if } 0 < r \le 1 \text{ and } 0 < \theta < 3\pi/2, \\ 0 & \text{else.} \end{cases}$$

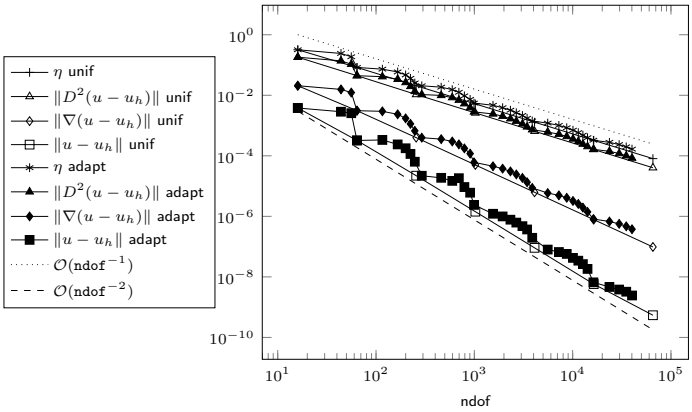

FIG. 1. *Convergence history in the smooth Experiment* 1 *for the BFS finite element.*

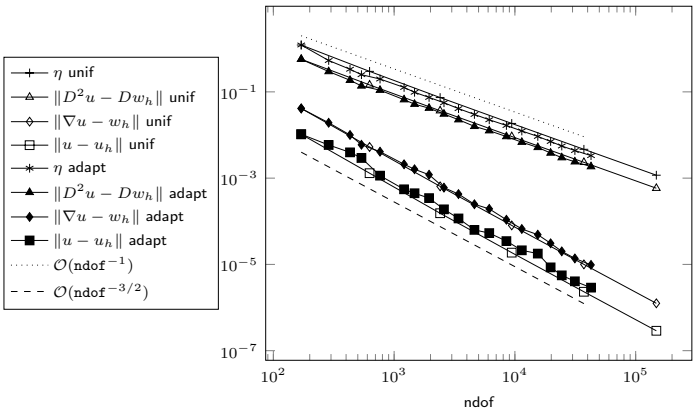

FIG. 2. *Convergence history in the smooth Experiment* 1 *for the Taylor–Hood finite element.*

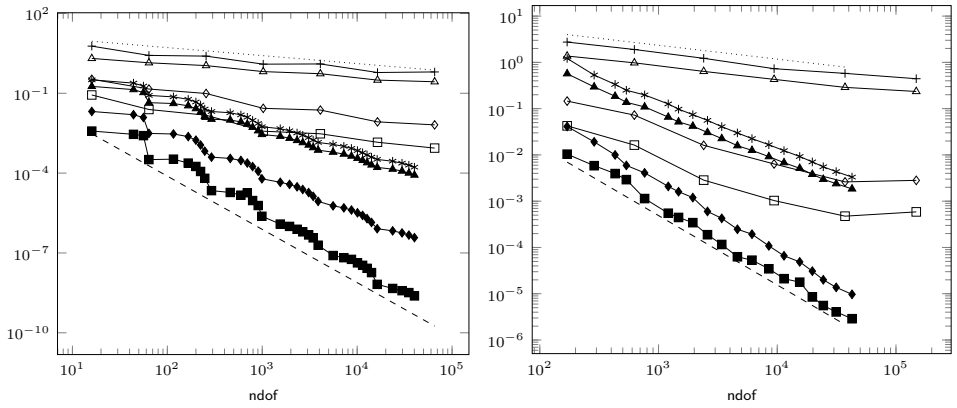

FIG. 3. *Convergence history in the smooth Experiment* 1 *with nonmatching initial mesh. Left: BFS method; cf. Figure* 1 *for a legend. Right: BFS method; cf. Figure* 2 *for a legend. In both plots, the dotted line indicates* $\mathcal{O}(\mathtt{ndof}^{-0.3})$ *(unlike in Figures* 1 and 2*).*

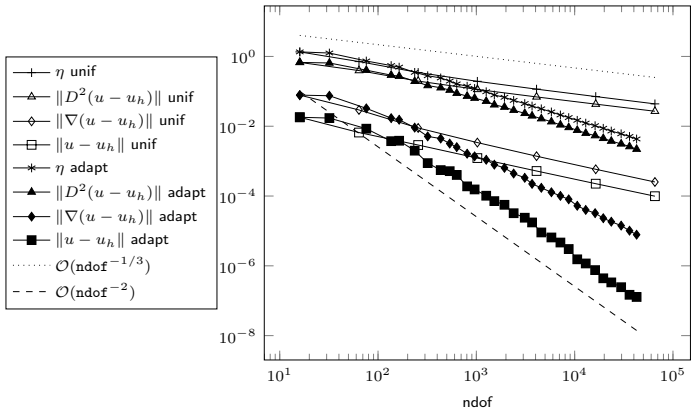

FIG. 4. *Convergence history in the singular Experiment* 2 *for the BFS finite element.*

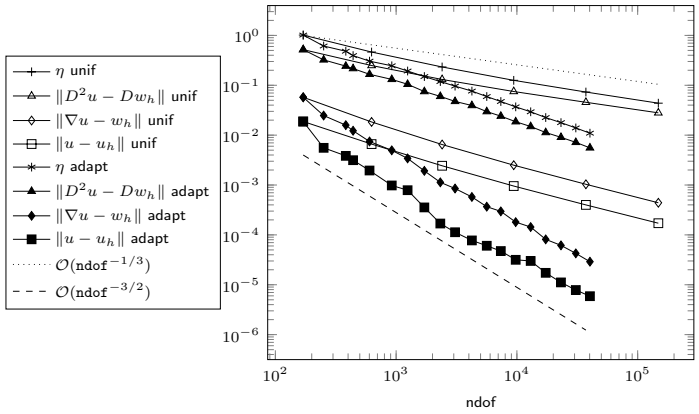

FIG. 5. *Convergence history in the singular Experiment* 2 *for the Taylor–Hood finite element.*

The Sobolev smoothness of u near the origin $(0,0)$ is strictly less than $H^{8/3}$. Also near the boundary of the sector $\{(r,\phi) : 0 < r < 1, 0 < \theta < 3\pi/2\}$ the regularity is reduced. The singularities in Experiment 2 lead to the suboptimal convergence rates of uniform refinement, displayed in the convergence history of Figure 4 for the BFS FEM and Figure 5 for the Taylor–Hood element. In both cases, the adaptive method converges at optimal rate. The graph of the solution computed with the adaptive BFS element and the adaptively generated meshes are displayed in Figure 6. In both cases, the refinement is pronounced in the regions where the solution is singular: the origin and the curved sector boundary.

5.5. Efficiency indices for Examples 1–2. The efficiency indices are defined by $\eta_{\mathrm{conf}}/\|D^2(u-u_h)\|_{L^2(\Omega)}$ for the conforming discretization and by $\eta_{\mathrm{mixed}}/\|D^2u - Dw_h\|_{L^2(\Omega)}$. Propositions 3.1 and 3.3 and the values of $\|A\|_{L^\infty(\Omega)}$ and $c(\gamma,\varepsilon)$, $c_\lambda^\tau(\gamma,\varepsilon)$, and $\sigma_\lambda^\tau(\gamma,\varepsilon)$, predict that the efficiency index ranges in the interval $[0.91886, 2]$ for the conforming discretization and in $[0.45943, 2.2186]$ for the mixed method. The efficiency indices for Experiments 1–2 with matching initial meshes are shown in Figure 7. For the conforming discretization they range from 1.6 to 2, while for the mixed scheme they lie between 1.5 and 2.2.

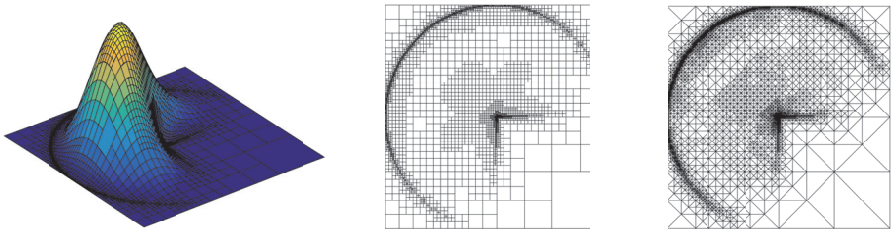

FIG. 6. *Experiment* 2. *Surface plot of the discrete BFS solution (left) and adaptive meshes. Middle: BFS,* 6017 *vertices,* 23,584 *degrees of freedom,* $\ell = 26$. *Right: Taylor–Hood,* 4518 *vertices,* 40,238 *degrees of freedom,* $\ell = 18$.

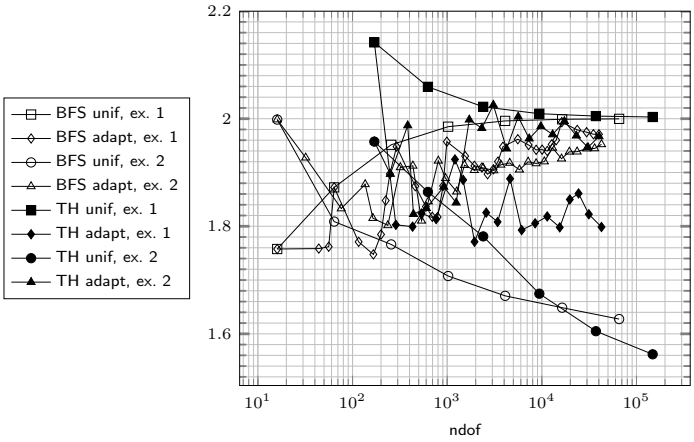

FIG. 7. *Efficiency indices (estimator/error) for the error estimators in Experiments* 1–2 *(BFS=Bogner–Fox–Schmit, TH=Taylor–Hood) with matching initial meshes.*

5.6. Experiment 3. This is an example with right-hand side $f = 1$, where the exact solution is unknown. The used coefficient is $A \circ \varphi$, that is, A is concatenated with the nonlinear transform $\varphi(x_1, x_2) = (x_1 + 1/3\ ,\ x_2 - 1/3 + (x_1 + 1/3)^{1/3})$. The coefficient is not aligned with the initial meshes and has a sharp discontinuity interface near the point $(-1/3, -1/3 + (1/3)^{1/3})$. Figure 8 displays the sign pattern of its off-diagonal entries. In Experiment 3, the meshes are not aligned with the discontinuous coefficient. The convergence history is shown in Figure 9 for the BFS method and the Taylor–Hood method. Since the exact solution is not known, the error estimators are plotted. In both cases, uniform refinement leads to the suboptimal convergence rate of $\mathcal{O}(\texttt{ndof}^{-0.35})$. The adaptive methods converge at a better rate. Still, it is suboptimal of rate $\mathcal{O}(\texttt{ndof}^{-1/2})$. This may be due to underintegration. Indeed, a Gaussian quadrature rule is used, which is not accurate for discontinuous function, and the adaptive method behaves like a first-order scheme. The adaptive meshes from Figure 8 show strong refinement toward the jump of the coefficient.

6. Conclusive remarks. The variational formulation of [21] as well as the new least-squares formulation of elliptic equations in nondivergence form can be discretized with conforming and, more importantly, mixed finite element technologies in a direct way. This allows for quasi-optimal error estimates and a posteriori error analysis. The proven convergence of the adaptive algorithm can be observed in the numerical

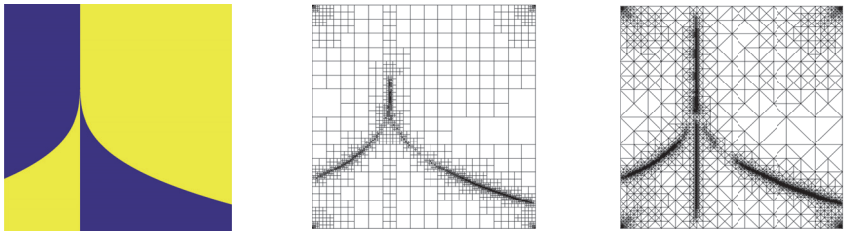

FIG. 8. *Experiment* 3 *with the nonmatching coefficient. Sign pattern of the off-diagonal entries of the coefficient A (left) and adaptive meshes. Middle: BFS,* 4808 *vertices,* 18,716 *degrees of freedom,* $\ell = 33$. *Right: Taylor–Hood,* 5848 *vertices,* 51,956 *degrees of freedom,* $\ell = 28$.

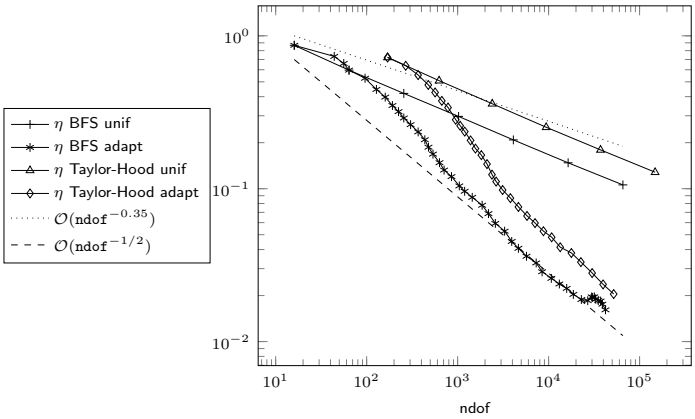

FIG. 9. *Convergence history for the BFS and the Taylor–Hood FEM for Experiment* 3 *with the nonmatching coefficient.*

experiments, and, as an empirical observation, appears to be quasi-optimal, provided the quadrature is accurate enough. The following remarks conclude this paper.

(a) *On the choice of the variational formulation.* The least-squares method is presented as an alternative approach to the nonsymmetric formulation of [21]. While the symmetry of the discrete problem is certainly a favorable property, a straightforward generalization to, e.g., Hamilton–Jacobi–Bellman equations (as presented in [22, 23] for the nonsymmetric formulation) is less obvious. This is due to the fact that the nonlinear operator in that problem does not have sufficient smoothness properties that would allow an analysis of a direct least-squares procedure. Alternatively, the least-squares method could be applied to the linear problems from a semismooth Newton algorithm. However, as semismoothness on the operator level does not hold in general (cf. [22, Rem. 1]), an analysis of this method requires further investigation.

(b) *Nonconvex domains.* The least-squares formulation may still be meaningful on nonconvex domains, but the solution will generally not coincide with that of (1).

(c) *Nonconforming schemes.* Nonconforming finite elements for fourth-order problems [5] have the advantage to be much simpler than their conforming counterparts. Since discrete analogues of (11) or (8) may not be satisfied without further stabilization terms, their application would require further modifications.

(d) *Lower-order terms.* Equations in nondivergence form including lower-order terms can be equally well treated in the proposed framework; see also [22]. The least-squares formulation can be derived from the minimization of the functional $\|A : D^2u + b \cdot \nabla u + cu - f\|_{L^2(\Omega)}$ for data b and $c > 0$. For the mixed system (16) this

leads to a coupling of (16a) and (16b)–(16c). The Cordes condition with lower-order terms [22] reads as follows: there exists $\alpha > 0$ such that

$$\big(|A|^2 + |b|^2/(2\alpha) + (c/\alpha)^2\big) \,/(\operatorname{tr} A + c/\alpha)^2 \leq 1/(d+\varepsilon).$$

More details on this Cordes condition are given in [22].

(e) *Space dimensions higher than $d = 3$.* The main arguments of this work are valid for any space dimension $d \geq 2$. Also the mixed formulation can be formulated in any dimension, provided it is posed in the space satisfying the constraint $\operatorname{rot} w = 0$, which in higher dimensions is understood as $Dw = (Dw)^*$. For the design of a numerical method, it remains to identify the space Q of multipliers.

Acknowledgments. The author thanks Prof. Ch. Kreuzer for a helpful discussion and the anonymous referees who helped to significantly improve the presentation.

REFERENCES

[1] P. Binev, W. Dahmen, and R. DeVore, *Adaptive finite element methods with convergence rates*, Numer. Math., 97 (2004), pp. 219–268.
[2] D. Boffi, F. Brezzi, and M. Fortin, *Mixed Finite Element Methods and Applications*, Springer Series in Comput. Math. 44, Springer, Berlin, 2013.
[3] D. Braess, *Finite Elements. Theory, Fast Solvers, and Applications in Elasticity Theory*, 3rd ed., Cambridge University Press, Cambridge, 2007.
[4] L. Caffarelli and L. Silvestre, *Smooth approximations of solutions to nonconvex fully nonlinear elliptic equations*, in Nonlinear Partial Differential Equations and Related Topics, Amer. Math. Soc. Transl. Ser. 2 299, AMS, Providence, RI, 2010, pp. 67–85.
[5] P. G. Ciarlet, *The Finite Element Method for Elliptic Problems*, Stud. Math. Appl. 4, North Holland, Amsterdam, 1978.
[6] H. O. Cordes, *Über die erste Randwertaufgabe bei quasilinearen Differentialgleichungen zweiter Ordnung in mehr als zwei Variablen*, Math. Ann., 131 (1956), pp. 278–312.
[7] M. Costabel and M. Dauge, *Maxwell and Lamé eigenvalues on polyhedra*, Math. Methods Appl. Sci., 22 (1999), pp. 243–258.
[8] W. Dörfler, *A convergent adaptive algorithm for Poisson's equation*, SIAM J. Numer. Anal., 33 (1996), pp. 1106–1124.
[9] X. Feng, L. Hennings, and M. Neilan, *Finite element methods for second order linear elliptic partial differential equations in non-divergence form*, Math. Comp., (2017), https://doi.org/10.1090/mcom/3168.
[10] X. Feng, M. Neilan, and S. Schnake, *Interior Penalty Discontinuous Galerkin Methods for Second Order Linear Non-divergence Form Elliptic PDEs*, arXiv:1605.04364, 2016.
[11] D. Gallistl, *Stable splitting of polyharmonic operators by generalized Stokes systems*, Math. Comp., (2017), https://doi.org/10.1090/mcom/3208.
[12] V. Girault and P.-A. Raviart, *Finite Element Methods for Navier–Stokes Equations. Theory and Algorithms*, Springer, Berlin, 1986.
[13] P. Grisvard, *Elliptic Problems in Nonsmooth Domains*, Monogr. Stud, Math. 24, Pitman, Boston, 1985.
[14] O. Lakkis and T. Pryer, *A finite element method for second order nonvariational elliptic problems*, SIAM J. Sci. Comput., 33 (2011), pp. 786–801.
[15] Z. Lou and A. McIntosh, *Hardy space of exact forms on $\mathbb{R}^N$*, Trans. Amer. Math. Soc., 357 (2005), pp. 1469–1496.
[16] A. Maugeri, D. K. Palagachev, and L. G. Softova, *Elliptic and Parabolic Equations with Discontinuous Coefficients*, Wiley, Berlin, 2000.
[17] P. Morin, K. G. Siebert, and A. Veeser, *A basic convergence result for conforming adaptive finite elements*, Math. Models Methods Appl. Sci., 18 (2008), pp. 707–737.
[18] R. H. Nochetto, K. G. Siebert, and A. Veeser, *Theory of Adaptive Finite Element Methods: An Introduction*, in Multiscale, Nonlinear and Adaptive Approximation, Springer, Berlin, 2009, pp. 409–542.
[19] R. H. Nochetto and W. Zhang, *Discrete ABP estimate and convergence rates for linear elliptic equations in non-divergence form*, Found. Comput. Math., (2017), https://doi.org/10.1007/s10208-017-9347-y.

[20] M. V. Safonov, *Nonuniqueness for second-order elliptic equations with measurable coefficients*, SIAM J. Math. Anal., 30 (1999), pp. 879–895.
[21] I. Smears and E. Süli, *Discontinuous Galerkin finite element approximation of nondivergence form elliptic equations with Cordès coefficients*, SIAM J. Numer. Anal., 51 (2013), pp. 2088–2106.
[22] I. Smears and E. Süli, *Discontinuous Galerkin finite element approximation of Hamilton–Jacobi–Bellman equations with Cordes coefficients*, SIAM J. Numer. Anal., 52 (2014), pp. 993–1016.
[23] I. Smears and E. Süli, *Discontinuous Galerkin finite element methods for time-dependent Hamilton–Jacobi–Bellman equations with Cordes coefficients*, Numer. Math., 133 (2016), pp. 141–176.
[24] R. Verfürth, *A Posteriori Error Estimation Techniques for Finite Element Methods*, Numer. Math. Sci. Comput., Oxford University Press, Oxford, 2013.